AIAA JOURNAL
Vol. 48, No. 6, June 2010

# Technical Notes

## Pitch, Roll, and Yaw Damping of a Flapping Wing

Shigeru Sunada, Yuki Hatayama, and Hiroshi Tokutake
*Osaka Prefecture University, Osaka, 599-8531, Japan*

DOI: 10.2514/1.J050098

### Nomenclature

| | | |
|---|---|---|
| $a$ | = | lift slope |
| $C$ | = | damping coefficient |
| $C_d$ | = | drag coefficient |
| $c$ | = | chord length of the wing |
| $\bar{c}$ | = | mean chord length |
| $F$ | = | tension of the thread |
| $f$ | = | flapping frequency |
| $g$ | = | gravitational acceleration |
| $h$ | = | distance between the tip path plane and the center of gravity |
| $I$ | = | moment of inertia of the total system (i.e., the flapping-wing aircraft, suspension bar, and counterbalancing weights) |
| $K$ | = | a constant in Eq. (2) |
| $L$ | = | rolling moment |
| $L_p$ | = | roll damping of the flapping-wing aircraft |
| $l$ | = | distance between the two threads used to suspend a bar attached to the $X$-flapping-wing aircraft |
| $l_s$ | = | length of each of two threads used to suspend a bar attached to the flapping-wing aircraft |
| $M$ | = | pitching moment |
| $M_q$ | = | pitch damping of the flapping-wing aircraft |
| $m$ | = | total mass of the flapping-wing aircraft, suspension bar, and counterbalancing weight |
| $m_a$ | = | mass of the flapping-wing aircraft |
| $m_w$ | = | mass of one wing |
| $N$ | = | yawing moment |
| $N_{\bar{r}}$ | = | yaw damping of the flapping-wing aircraft |
| $P$ | = | cycle period of rotation |
| $p$ | = | roll rate |
| $q$ | = | pitch rate |
| $R$ | = | wing length |
| $r$ | = | spanwise position |
| $r$ | = | yaw rate |
| $S_w$ | = | area of one wing |
| $t$ | = | time |
| $T$ | = | thrust |
| $v_i$ | = | induced velocity |
| $\beta$ | = | flapping angle |
| $\beta_0$ | = | mean flapping angle |
| $\bar{\beta}$ | = | amplitude of flapping motion |
| $\Theta$ | = | rotational angle |
| $\Theta_0$ | = | initial rotational angle |
| $\bar{\Theta}$ | = | amplitude of the rotational motion |
| $\theta$ | = | feathering angle |
| $\bar{\theta}$ | = | amplitude of feathering motion |
| $\rho$ | = | density of air |
| $\Phi$ | = | angle of the thread measured from the vertical direction of the gravitational force |

*Subscripts*

| | | |
|---|---|---|
| 1, 2 | = | cases 1 and 2, respectively |
| right, left | = | right and left wing, respectively |
| $u$, $l$ | = | upper and lower wing, respectively |

Received 25 July 2009; revision received 30 December 2009; accepted for publication 9 February 2010. 

### Introduction

RECENTLY, centimeter-sized flapping-wing micro air vehicles have been studied [1–4]. The motivation of these studies is probably that a flapping wing is successful in nature for creatures on this scale. The University of Toronto [5] and Aerovironment* developed flapping-wing micro air vehicles that can hover. The stability of the attitude is the most important requirement for a hovering flapping-wing air vehicle. In this study, we measured the three major indicators of vehicle stability for a flapping-wing aircraft while hovering: roll, pitch, and yaw damping. Figure 1 shows the axes of rolling, pitching, and yawing motions. For a hover flight, the axes are defined so that the tip path plane is horizontal. In addition, equations for the roll, the pitch, and the yaw damping are established and the values from the equations were compared with the experimental ones.

### Experiments

#### Flapping Aircraft Used in the Experiment

A toy model ornithopter (R/C Dragonfly, Wow Wee Corp.)† was used in the measurements (Fig. 1). Table 1 lists the physical characteristics of this flapping-wing aircraft, which has two pairs of wings arranged in an $X$ configuration. Each wing is made of two carbon spars and a vinyl sheet and has a schematic planform (Fig. 2). Note that only one carbon spar is connected to the wing hub and the other is not connected to the previous carbon spar and the wing hub. The four wings flap on one plane, and the flapping motion of the left and the right wings are symmetric about the center plane. The flapping and feathering motions are expressed by

$$\beta = \beta_0 + \frac{\bar{\beta}}{2}\cos(2\pi f t), \qquad \theta = \frac{\pi}{2} - \frac{\bar{\theta}}{2}\sin(2\pi f t) \tag{1}$$

The values of $\beta_0$, $\bar{\beta}$, and $\bar{\theta}$ of the upper and lower wings are shown in Table 1. When $t = 0$, $\beta_l \approx \beta_u$. The upper and lower wings generate a clap-fling motion [6]. The distance from point O to the flapping plane swept by the spars on leading edge $h$ was 12 cm.

Figure 3a shows the time variation in the feathering angle of upper wing $\theta_u$ when $f = 9.2$ Hz and 7.1 Hz. Figure 3b schematically defines $\theta_u$ and $\theta_l$ based on view A in Fig. 1. $\theta_u$ and $\theta_l$ were measured at midspan, and $\theta_l \approx \pi - \theta_u$. When the roll, pitch, and yaw damping was measured, as indicated in Table 2, the values of $f$ are between the two values of $f$ in Fig. 3a.

*Data available online at http://www.avav.com/uas/adc/nano/ [retrieved 29 December 2009].

†Data available online at http://www.flytechonline.com/ [retrieved 29 December 2009].

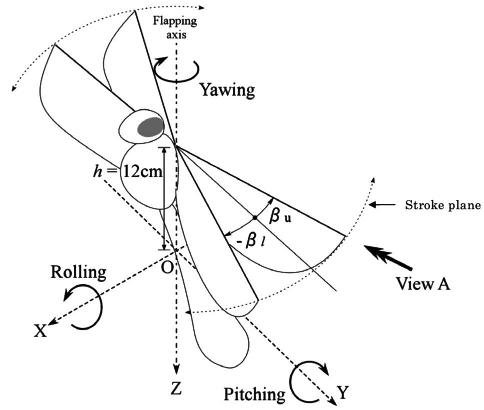


**Fig. 1 Schematic of *X*-flapping-wing aircraft (R/C Dragonfly, toy model ornithopter, Wow Wee Corp.), showing rolling, pitching, and yawing axes and flapping angles $\beta_u$ and $\beta_l$.**

### Experimental Apparatus

Figure 4 shows the experimental apparatuses. The bar was suspended by two threads of length $l_s = 800$ mm and distance $l$ apart (Table 2). The flapping aircraft was attached on the bar. The bar was placed along the $Y$ and $Z$ axes to measure the roll/yaw and pitch damping, respectively. Note the $X$ and $Z$ axes were vertical, when the roll and yaw damping was measured, respectively. The center of the bar is in accordance with point O on the flapping-wing aircraft.

The roll, pitch, and yaw damping of the flapping-wing aircraft was measured as follows: the rotational angle of bar $\Theta$ was set by hand at $\Theta_0$ around the $X$, $Y$, and $Z$ axes for measuring the roll, pitch, and yaw damping, respectively. Weights were then mounted as a counterbalance at certain positions along the bar so that point O did not move when the bar was rotated about the rotational axis, which is through point O.

When the bar was released by hand, the bar with the attached flapping-wing aircraft started rotating around the $X$, $Y$, and $Z$ axes. Time variation in $\Theta$ was determined based on the images of these rotational motions obtained by video camera. The measurements for each damping were just taken for two cases of motion: 1) case 1, when the wings made flapping motions, and 2) case 2, when the wings were folded and the wing area was thus close to 0. The damping due to the flapping wings was obtained by comparing the results for cases 1 and 2.

## Analysis of Experimental Results

The dynamics of the rotational motion of the bar with the flapping-wing aircraft were evaluated as follows. When $\Theta$, $\Phi \ll 1$, the following equation of motion is obtained:

$$I\ddot{\Theta} + C\dot{\Theta} + \frac{(mg + KT)l^2}{4l_s}\Theta = 0 \tag{2}$$

where $K$ is a parameter that is 1 for case 1 of the measurement of the yaw damping and 0 in all other cases.

**Table 1 Physical characteristics of *X*-flapping-wing aircraft**

| Items | Values |
|---|---|
| Mass of aircraft, $m_a$, g | 23.9 |
| Number of wings, $b$ | 4 |
| Wing length, $R$, cm | 20.5 |
| Averaged chord length of wing, $\bar{c}$, cm | 7.7 |
| Mass of wing, $m_w$, g | 1.06 |
| Area of wing, $S_w$, m$^2$ | $1.57 \times 10^{-2}$ |
| Flapping angle of upper wing, $\beta_u$ | $25.0° - 20.4° \cos(2\pi\ \mathrm{ft})$ |
| Flapping angle of lower wing, $\beta_l$ | $-16.5° + 21.1° \cos(2\pi\ \mathrm{ft})$ |

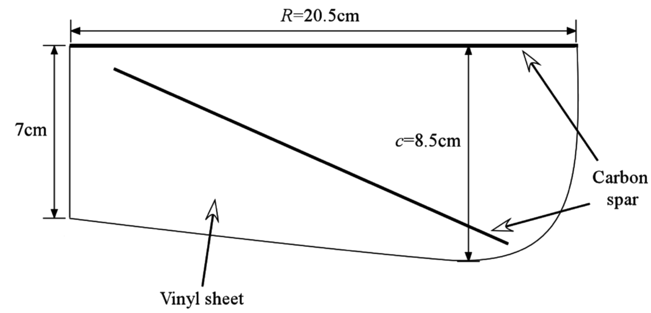


**Fig. 2 Planform of wing for *X*-flapping-wing aircraft.**

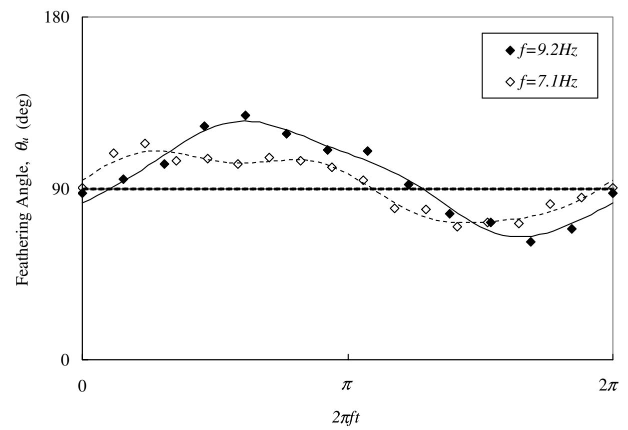


**a)**

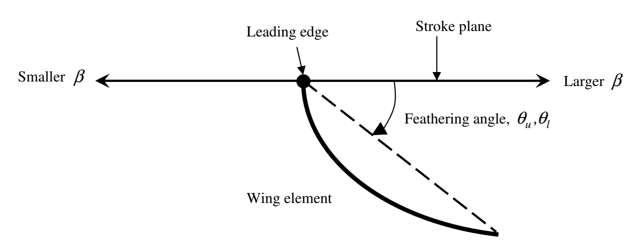


**b)**

**Fig. 3 Feathering angle measured at midspan of upper wing: a) time variation of feathering angles $\theta_u$, $\theta_l$ when flapping frequency $f = 9.2$ Hz and 7.1 Hz; b) definition of feathering angle based on view A in Fig. 1.**

The solution of Eq. (2) is given by

$$\Theta = \Theta_0 \exp\left(\frac{-C}{2I}t\right)\cos\left(\frac{\sqrt{-C^2 + Il^2(mg + KT)/l_s}}{2I}t\right)$$
$$\equiv \bar{\Theta}\cos\left(\frac{\sqrt{-C^2 + Il^2(mg + KT)/l_s}}{2I}t\right) \tag{3}$$

With obtained $\Theta(t)$, the value of $-C/2I$ and the period of rotational motion $P \equiv 4\pi I/\sqrt{-C^2 + Il^2(mg + KT)/l_s}$ can be obtained. Then the values of $C$ and $I$ can be estimated from the values of $-C/2I$ and $P$.

## Theory

Here the equations for roll, pitch, and yaw damping by one pair of right and left wings are established, based on the blade element theory. During the downstroke, the aerodynamic moments around the $X$ axis acting on the right and left wings due to rolling motion $p$ are given, respectively, by

**Table 2 Experimental parameters and measured roll, pitch, and yaw damping for *X*-flapping-wing aircraft**

| | $f$, Hz | $T$, N | $m$, kg | $l$, m | $P$, sec | $I$, kgm$^2$ | $C$, Nms | Damping, Nms |
|---|---|---|---|---|---|---|---|---|
| roll | 8.4 | 0.22 | 0.31 | 0.3 | $P_1 = 1.2$ | $I_1 = 3.07 \times 10^{-3}$ | $C_1 = 1.47 \times 10^{-3}$ | $L_p = -1.37 \times 10^{-3}$ |
| | | | | | $P_2 = 1.2$ | $I_2 = 3.08 \times 10^{-3}$ | $C_2 = 1.00 \times 10^{-4}$ | |
| pitch | 7.4 | 0.18 | 0.38 | 0.3 | $P_1 = 1.1$ | $I_1 = 3.38 \times 10^{-3}$ | $C_1 = 8.08 \times 10^{-4}$ | $M_q = -7.32 \times 10^{-4}$ |
| | | | | | $P_2 = 1.1$ | $I_2 = 3.29 \times 10^{-3}$ | $C_2 = 7.63 \times 10^{-5}$ | |
| yaw | 7.2 | 0.15 | 0.25 | 0.56 | $P_1 = 1.0$ | $I_1 = 6.60 \times 10^{-3}$ | $C_1 = 2.61 \times 10^{-3}$ | $N_{\bar{r}} = -2.38 \times 10^{-3}$ |
| | | | | | $P_2 = 1.1$ | $I_2 = 6.75 \times 10^{-3}$ | $C_2 = 2.31 \times 10^{-4}$ | |

$$
\begin{aligned}
L_{\mathrm{right}} &= -\frac{\rho}{2}\int_0^R \{(r\dot{\beta})^2 + (pr - v_i)^2\} ca \left(\theta + \frac{pr - v_i}{-r\dot{\beta}}\right) r\,\mathrm{d}r \\
L_{\mathrm{left}} &= \frac{\rho}{2}\int_0^R \{(r\dot{\beta})^2 + (pr + v_i)^2\} ca \left(\theta - \frac{pr + v_i}{-r\dot{\beta}}\right) r\,\mathrm{d}r
\end{aligned}
\tag{4}
$$

On the other hand, during the up stroke, they are given by

$$
\begin{aligned}
L_{\mathrm{right}} &= -\frac{\rho}{2}\int_0^R \{(r\dot{\beta})^2 + (pr - v_i)^2\} ca \left(\pi - \theta + \frac{pr - v_i}{r\dot{\beta}}\right) r\,\mathrm{d}r \\
L_{\mathrm{left}} &= \frac{\rho}{2}\int_0^R \{(r\dot{\beta})^2 + (pr + v_i)^2\} ca \left(\pi - \theta - \frac{pr + v_i}{r\dot{\beta}}\right) r\,\mathrm{d}r
\end{aligned}
\tag{5}
$$

The aerodynamic moment due to one pair of wings, which is averaged during one cycle, is given by

$$
L = -p\rho a|\bar{\beta}| f \bar{c}\frac{R^4}{2} \tag{6}
$$

Here, it is assumed that $(r\dot{\beta})^2 + (pr \pm v_i)^2 \simeq (r\dot{\beta})^2$. Then roll damping is

$$
L_p = -\rho a|\bar{\beta}| f \bar{c}\frac{R^4}{2} \tag{7}
$$

During the downstroke, the aerodynamic moments around the $Y$ axis acting on the right and left wings due to pitching motion $q$ are given by

$$
\begin{aligned}
M_{\mathrm{right}} = M_{\mathrm{left}} &= -\frac{\rho}{2}\int_0^R \{(r\dot{\beta} + hq)^2 + (-qr\sin\beta + v_i)^2\} ca \\
&\quad \times \left(\theta - \frac{-qr\sin\beta + v_i}{-r\dot{\beta} - hq}\right) r\sin\beta\,\mathrm{d}r
\end{aligned}
\tag{8}
$$

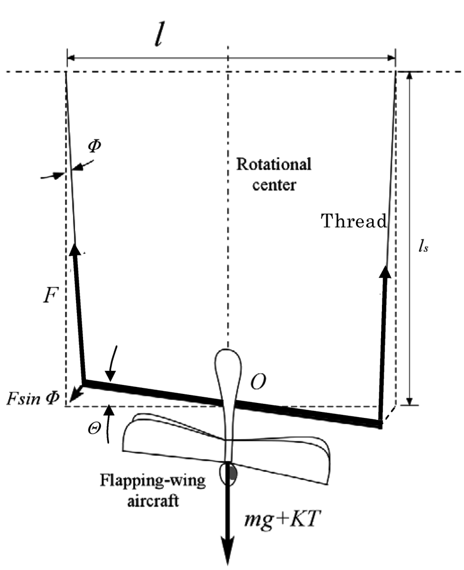


**Fig. 4 Experimental apparatus; this figure shows how the aircraft is suspended for measuring yaw damping.**

On the other hand, during the up stroke, they are given by

$$
\begin{aligned}
M_{\mathrm{right}} = M_{\mathrm{left}} &= -\frac{\rho}{2}\int_0^R \{(r\dot{\beta} + hq)^2 + (-qr\sin\beta + v_i)^2\} ca \\
&\quad \times \left(\pi - \theta - \frac{-qr\sin\beta + v_i}{r\dot{\beta} + hq}\right) r\sin\beta\,\mathrm{d}r
\end{aligned}
\tag{9}
$$

The aerodynamic moment due to one pair of wings, which is averaged during one cycle, is given by

$$
\begin{aligned}
M &= -\frac{\pi}{4}\rho a\bar{c}R^4 f^2 \left[\bar{\beta}^2\beta_0\left\{\left(\frac{\pi}{2}\right)^2 - \frac{2}{3}\bar{\theta}\right\}\right] \\
&\quad - \frac{\rho}{2}a\bar{c}R^4 f\left(|\bar{\beta}|\beta_0^2 + \frac{\bar{\beta}^3}{12}\right) q + \frac{2\rho}{3}a\bar{c}R^3 f v_i |\bar{\beta}|\beta_0 \\
&\quad - \frac{\rho}{2}a\bar{c}R^2\left\{\beta_0\left(\frac{\pi}{2} - \frac{\bar{\theta}}{\pi}\right)\right\} h^2 q^2
\end{aligned}
\tag{10}
$$

Here, it is assumed that $(r\dot{\beta} + hq)^2 + (-qr\sin\beta + v_i)^2 \simeq (cr\dot{\beta} + hq)^2$. Therefore, pitch damping is

$$
M_q = -\frac{\rho}{2}a\bar{c}R^4 f\left(|\bar{\beta}|\beta_0^2 + \frac{\bar{\beta}^3}{12}\right) - \rho a\bar{c}R^2 h^2\left\{\beta_0\left(\frac{\pi}{2} - \frac{\bar{\theta}}{\pi}\right)\right\} q \tag{11}
$$

When the wing motion is not symmetrical about $Y$-$Z$ plane, that is, $\beta_0 \neq 0$, the second term in Eq. (11) is not equal to zero. In the present experiments, pitching motion is periodic. The time-averaged value of $M_q$, which is obtained in this experiment, is

$$
M_q = -\frac{\rho}{2}a\bar{c}R^4 f\left(|\bar{\beta}|\beta_0^2 + \frac{\bar{\beta}^3}{12}\right) \tag{12}
$$

During the downstroke, aerodynamic moments around the $Z$ axis acting on the right and left wings due to yawing motion $\bar{r}$ are, respectively, given by

$$
\begin{aligned}
N_{\mathrm{right}} &= \frac{\rho}{2}\int_0^R \{r^2(\dot{\beta} + \bar{r})^2 + v_i^2\} crC_d\,\mathrm{d}r \\
N_{\mathrm{left}} &= -\frac{\rho}{2}\int_0^R \{r^2(-\dot{\beta} + \bar{r})^2 + v_i^2\} crC_d\,\mathrm{d}r
\end{aligned}
\tag{13}
$$

Here, $C_d$ is assumed to be a constant. And it is assumed that $v_i^2 < r^2(\dot{\beta} + \bar{r})^2$ and $v_i^2 < r^2(-\dot{\beta} + \bar{r})^2$ for the right and left wing, respectively. Then, the yawing moment due to lift acting on the wing can be ignored. During the up stroke, aerodynamic moments around the $Z$ axis acting on the right and left wings due to yawing motion $\bar{r}$ are, respectively, given by

$$
\begin{aligned}
N_{\mathrm{right}} &= -\frac{\rho}{2}\int_0^R \{r^2(\dot{\beta} + \bar{r})^2 + v_i^2\} crC_d\,\mathrm{d}r \\
N_{\mathrm{left}} &= \frac{\rho}{2}\int_0^R \{r^2(-\dot{\beta} + \bar{r})^2 + v_i^2\} crC_d\,\mathrm{d}r
\end{aligned}
\tag{14}
$$

The aerodynamic moment due to one pair of wings, which is averaged during one cycle, is given by

$$
N = -\bar{r}\rho C_d \bar{c}R^4 f|\bar{\beta}| \tag{15}
$$

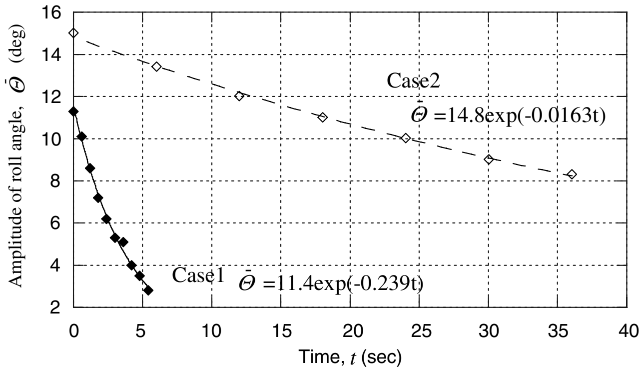


**Fig. 5 Measured roll angle of *X*-flapping-wing aircraft.**

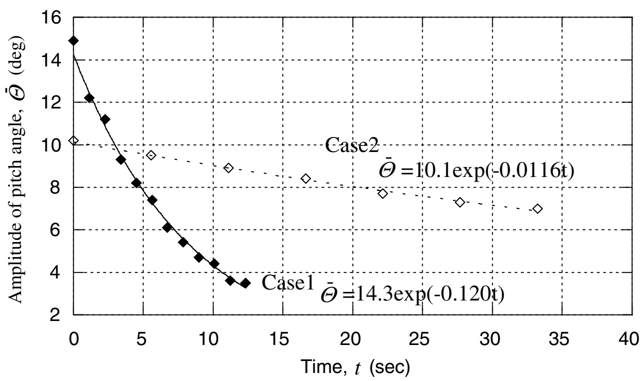


**Fig. 6 Measured pitch angle of *X*-flapping-wing aircraft.**

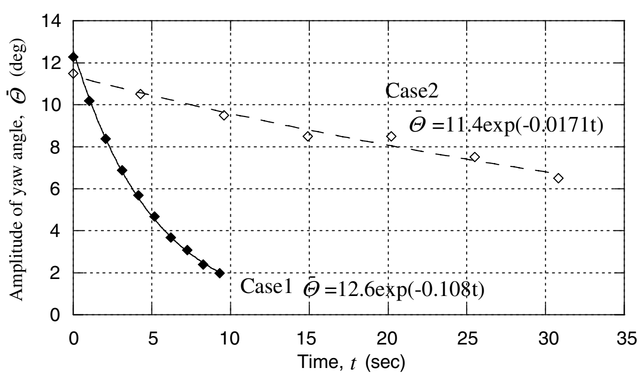


**Fig. 7 Measured yaw angle of *X*-flapping-wing aircraft.**

Then yaw damping is

$$N_{\bar{r}} = -\rho C_d \bar{c} R^4 f |\bar{\beta}| \tag{16}$$

## Results

Figures 5–7 show the time variations in amplitude $\bar{\Theta}$ of the roll, pitch, and yaw angle, respectively. The values of $-C/2I$ are shown in the equations ($\bar{\Theta} = \Theta_0 \exp\{(-C/2I)t\}$) indicated in these figures. Table 2 shows the values of $f$, $T$, $m$, and $l$ used in the measurements. The values of $C$ and $I$ (Table 2) were obtained based on the values of $-C/2I$ in Figs. 5–7 and those of $P$ in Table 2. In the measurements, $I_1 \approx I_2$. These results suggest that the moment of inertia of the wings was much smaller than that of the total system. The values of $-(C_1 - C_2)$ indicate the roll, pitch, and yaw damping due to the flapping wings: $L_p$, $M_q$ and $N_r$, respectively.

Table 3 compares roll, pitch, and yaw damping between the measurements and the analysis.

**Table 3 Comparison of roll, pitch, and yaw damping between measurements and analysis**

| | Damping obtained by measurements, Nms | Damping obtained by analysis, Nms |
|---|---|---|
| Roll | $L_p = -1.4 \times 10^{-3}$ | $L_p = -2.5 \times 10^{-3}$ |
| Pitch | $M_q = -7.3 \times 10^{-4}$ | $M_q = -3.9 \times 10^{-4}$ |
| Yaw | $N_{\bar{r}} = -2.4 \times 10^{-3}$ | $N_{\bar{r}} = -2.4 \times 10^{-3}$ |

In the calculations of roll and pitch damping, lift slope $a$ was assumed to be 2.5, so that the differences between the experimental damping and the theoretical ones are small. Similarly, in the calculation of yaw damping, drag coefficient $C_d$ was assumed to be 1.4. These assumed values include the error from the approximations for obtaining Eqs. (7), (12), and (16). Note that the induced velocity is not in these equations.

## Conclusions

Equations for the roll, pitch, and yaw damping of a flapping-wing aircraft while hovering are established, based on the blade element theory. The roll, pitch, and yaw damping of an *X*-flapping-wing aircraft while hovering was measured. Comparisons between experimental and theoretical values showed the small differences. Note that the lift slope and drag coefficient were assumed to be 2.5 and 1.4, respectively.

The Lock number [7] of the wings of the flapping-wing aircraft is 70.6. This value, which is much larger than that of a helicopter, reflects the small mass of the flapping wing. Wings with such small Lock numbers cannot be used as a helicopter rotor. In our analysis, we ignored the deformation of the wings out of the stroke plane because the carbon spar on the leading edge is so rigid that its bending deformation is small. This is different from the roll and pitch damping of a helicopter that strongly depends on the deformation/motion of a wing out of the stroke plane (for a helicopter, this plane is called the tip path plane), which is called the flapping motion for a helicopter.

## References

[1] Singh, B., and Chopra, I., "Insect-Based Hover-Capable Flapping Wings for Micro Air Vehicles: Experiments and Analysis," *AIAA Journal*, Vol. 46, No. 9, 2008, pp. 2115–2135.
[2] Rosenfeld, N. C., and Wereley, N. M., "Time-Periodic Stability of a Flapping Insect Wing Structure in Hover," *Journal of Aircraft*, Vol. 46, No. 2, 2009, pp. 450–464.
[3] Rakotomamonjy, T., Ouladsine, M., amd Moing, T. L., "Modelization and Kinematics Optimization for a Flapping-Wing Micro Air Vehicle," *Journal of Aircraft*, Vol. 44, No. 1, 2007, pp. 217–231.
[4] Warkentin, J., and DeLaurier, J., "Experimental Aerodynamics Study of Tandem Flapping Membrane Wings," *Journal of Aircraft*, Vol. 44, No. 5, 2007, pp. 1653–1661.
[5] Zdunich, P., Bilyk, D., MacMaster, M., Loewen, D., DeLaurier, J., Kornbluh, R., Low, T., Stanford, S., and Holeman, D., "Development and Testing of the Mentor Flapping-Wing Micro Air Vehicle," *Journal of Aircraft*, Vol. 44, No. 5, 2007, pp. 1701–1711.
[6] Weis Fogh, T., "Quick Estimates of Flight Fitness in Hovering Animals, Including Novel Mechanisms for Lift Production," *Journal of Experimental Biology*, Vol. 59, 1973, pp. 169–230.
[7] Johnson, W., *Helicopter Theory*, Dover, New York, 1980.

E. Livne
*Associate Editor*